IRSTI 29.19.31 https://doi.org/10.26577/phst20251225

$ZnCo_2O_4$ nanostructure-based electrochemical sensor for highly sensitive glucose detection

L.V. Gritsenko[1, 2]*, Zh.K. Kalkozova[1, 3], Y.Y. Kedruk[4], Zh.U. Paltusheva[2], M.N. Mussakhanov[4] and Kh.A. Abdullin[1, 3]

[1]Institute of Applied Sciences and Information Technologies, Almaty, Kazakhstan
[2]Satbayev University, Almaty, Kazakhstan
[3]National Nanotechnology Laboratory of Open Type, Al-Farabi Kazakh National University, Almaty, Kazakhstan
[4]Kazakh-British Technical University, Almaty, Kazakhstan
*e-mail: l.gritsenko@satbayev.university

(Received August 22, 2025; received in revised form November 16, 2025; accepted November 30, 2025)

Enzyme-free electrochemical glucose sensors attract the attention of researchers due to their high reproducibility and stability compared to enzymatic sensors, which is of practical importance for both clinical diagnostics and the food industry. The development of an economical, controlled method for the synthesis of a multicomponent composite used to determine glucose is an urgent task for the prevention and treatment of diabetes. In this work, zinc cobaltite $ZnCo_2O_4$ nanostructures on nickel foam were synthesized using a simple hydrothermal method. The possibility of using the grown structures as a basis for enzyme-free electrochemical sensors for determining glucose is shown. It was revealed that the concentration of the growth solution affects the morphology of the synthesized structures and their electrochemical properties. The highest sensitivity to glucose 18.65 $mA \cdot mM^{-1} \cdot cm^{-2}$ in an alkaline solution of 0.1 M KOH was demonstrated by $ZnCo_2O_4$ samples grown in an aqueous solution containing 40 mM zinc nitrate and 400 mM cobalt nitrate. The results of the study show that the molar predominance of cobalt nitrate in the growth solution contributes to an increase in the electrochemical sensitivity of Ni-$ZnCo_2O_4$ electrodes. The obtained samples can be used as highly sensitive electrodes used both in medical applications and for the needs of the food industry.

Keywords: nanostructured composites, electrochemical biosensor, hydrothermal method, glucose, cyclic voltammetry, oxide semiconductors.
PACS number(s): 61.46.+w, 61.46.−w, 61.82.Fk, 68.37.Lp, 81.07.Bc, 81.10.Dn, 82.47.Rs.

1. Introduction

Diabetes, a serious chronic disease, is a public health problem. The number of recorded cases of this disease is steadily increasing. In this regard, the development of efficient, cost-effective, and highly glucose-sensitive biosensors is an urgent task [1-5]. Due to instability, high cost and complexity of immobilization in the development of enzyme sensors, the development of enzyme- free glucose sensors attract special interest of researchers [6-9]. Nanostructured noble metals such as Pt, Au, etc. are actively used for non-enzymatic glucose sensing [10-13]. The disadvantage of these sensors is that some noble metals are easily poisoned by intermediates formed during glucose oxidation, as well as chlorine ions in the test solution. An alternative to noble metals for glucose electrooxidation is transition metal nanostructures and their oxides, which are promising due to their large surface area, low cost, and unique electrocatalytic properties [14-16]. In particular, bimetallic oxide $NiCo_2O_4$ has been actively used because of its high electrical conductivity as well as high electrocatalytic activity compared to single metal oxides such as NiO, Co_3O_4 and CuO [17-20]. However, disadvantages such as brittle structure, easy self-agglomeration and dissolution on the electrode surface make it very difficult to use $NiCo_2O_4$ for glucose determination [17, 21 – 23].

Zinc cobaltite $ZnCo_2O_4$ is a well-known ternary spinel oxide possessing a high degree of cation disorder in two types of lattice sites tetrahedrally or octahedrally coordinated by oxygen [23]. It is a promising p-type functional material attracting considerable interest in potential applications such as lithium ion batteries, electrocatalysts, supercapacitors, etc. due to its electrochemical and catalytic properties [24-27]. In the $ZnCo_2O_4$ crystal Zn cations occupy tetrahedral positions, Co cations are uniformly distributed throughout the octahedral positions, and anions O_2 tend to coordinate both Zn^{2+} and Co^{3+} cations tetrahedrally and octahedrally, respectively, forming a closely packed structure [28, 29].

The fabrication of nanoparticle arrays is relevant in applications where important electrochemical processes take place. The morphology of the electrodes having a strong influence on their properties [30 – 34]. Nanostructured samples have enhanced reactivity and stability, providing pathways for electrolyte ions and electrons, thereby realizing maximum utilization of the electrochemical properties of the material [32 – 39]. The hydrothermal method is an inexpensive low-temperature synthesis method of nanostructured materials based on oxide semiconductors, which are promising for use in biosensors for solving healthcare problems, for chemical and biological analysis, monitoring of the ecological state of the environment, and in the food industry [9, 40]. To create a highly sensitive enzyme-free electrochemical sensor for the detection of glucose in alkaline solution, the use of nanostructured materials is promising [7, 14, 21, 22].

This paper presents the results of a study of the electrochemical properties of nanostructured composite materials based on $ZnCo_2O_4$ spinel synthesized by a low-cost hydrothermal method on nickel foam substrates. The study is aimed at assessing their potential as sensitive electrodes at electrochemical glucose (gl) detection.

2. Materials and methods

Zinc cobaltite samples were obtained by hydrothermal method on nickel foam. The growth solution contained cobalt nitrate $Co(NO_3)_2 \cdot 6H_2O$ (Sigma Aldrich, 99% purity), zinc nitrate $Zn(NO_3)_2 \cdot 6H_2O$ (Sigma Aldrich, 99% purity), and urea CH_4N_2O (Sigma Aldrich, 99% purity). Urea acts as a precipitating agent during hydrothermal synthesis. Six types of samples with different molar concentration ratios of zinc nitrate (NZn) / cobalt nitrate (NCo) are considered in this work: ZC1 (NZn40mM/NCo40mM), ZC2 (NZn60mM/NCo60mM), ZC3 (NZn40mM/NCo400mM), ZC4 (NZn60mM/NCo600mM), ZC5 (NZn400mM/NCo40mM), ZC6 (NZn600mM/NCo60mM) (see Table 1). The hydrothermal synthesis of nanostructures was carried out in a hermetically sealed autoclave at 140 °C for 4 hours. During the synthesis, the nickel foam substrate was placed vertically in the autoclave. At the end of the synthesis, all samples were washed with distilled water and air-dried at 80 °C.

The surface morphology of prepared samples was studied with transmission electron microscope (TEM, JEOL, JEM-1400 plus, Japan) (Fig. 1). The morphology of the sample ZC2 (NZn60mM/NCo60mM) presented in Figure 1a is characterised by nanoparticles in the form of plates or nanorods. The average particle size is of the order of 10-20 nm, which is characteristic of the formation of nanocrystalline spinel structure $ZnCo_2O_4$ during hydrothermal growth. A relatively homogeneous dispersion of crystallites is observed, indicating a close to stoichiometric ratio, as well as balanced conditions of nucleation and growth in solution at a molar ratio of Zn:Co = 1:1. This morphology is favourable for the formation of a developed specific surface area, which is critical for applications in sensing devices and electrochemical systems. Figure 1b shows a snapshot of sample ZC6 (NZn600mM/NCo60mM) synthesised at a precursor ratio of Zn:Co = 10:1. In contrast to sample ZC2, this material shows more pronounced aggregation and formation of larger crystallites (— 30-40 nm), indicating enhanced crystallite growth under zinc excess conditions. Apparently, high Zn^{2+} content leads to a change in the kinetics of hydrolysis and precipitation, while maintaining the nanocrystalline structure characteristic of spinels, but with a lower specific surface area compared to the ZC2 sample.

3. Results and discussion

Thus, by varying the molar ratios of Zn^{2+}/Co^{2+} in the growth solution, the morphology of $ZnCo_2O_4$ nanostructures can be controlled. At a stoichiometric ratio (1:1), the formation of uniform nanoparticles with high dispersion is observed, whereas at a significant excess of zinc (10:1), aggregation and crystallite growth are enhanced, leading to enlarged nanostructures.

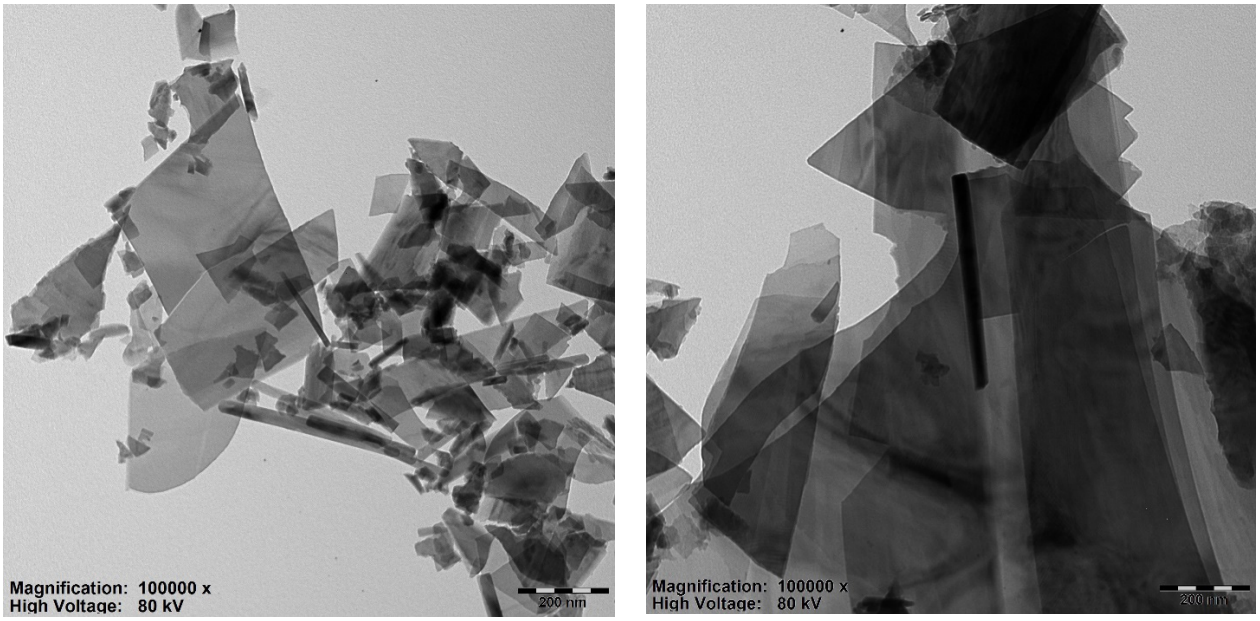

(a) (b)

Figure 1 – TEM of $ZnCo_2O_4$ samples: (a) ZC2, (b) ZC6.

The electrochemical properties of the obtained samples were investigated on a Corrtest CS310 single-channel potentiostat using a three-electrode electrochemical glass cell in 0.1M KOH alkaline solution at a scan rate of 25 mV/s. Cyclic voltammetry (CV) was measured at room temperature at potential changes from -0.1 to 0.65 V. An Ag/AgCl reference electrode was used for electrochemical measurements in a three-electrode setup.

The concentration of glucose in the alkaline solution varied from 0.2 mM to 2 mM. Figure 2 shows the CVs of the synthesized samples. It is observed that maximum oxidation currents are observed at ~0.6 V and maximum reduction currents are observed at ~0.3 V. The peaks of oxidation and reduction currents gradually increase with increasing concentration of glucose in solution.

The corresponding redox potentials indicate that the synthesised material is $ZnCo_2O_4$ [41]. It is observed that the anodic and cathodic peak potentials shift to the positive and negative side, respectively, with increasing glucose concentration in solution, indicating increasing concentration polarization.

The most pronounced anodic currents are observed for samples ZC3 and ZC4 synthesised at excess of cobalt ions (Zn:Co = 1:10). In particular, sample ZC3 (Zn:Co = 40:400 mM) exhibits the highest anodic current upon addition of glucose, indicating high catalytic activity. In contrast, the samples with excess zinc (ZC5 and ZC6) show significantly weaker current responses, indicating that the catalytic efficiency decreases as the proportion of Zn^{2+} in the growth solution increases. To compare the sensitivity of the samples, calibration plots were constructed for the oxidation current peaks as a function of glucose concentration in solution (Figure 3). On the graph R^2=0.99, linear range 0–2 mM. All dependences have a linear character in the investigated range, which confirms the suitability of these materials for quantitative determination of glucose.

On the basis of these dependences the sensitivity of each sample was calculated (Table 1). It was observed that the highest sensitivity (18.65 $mA \cdot mM^{-1} \cdot cm^{-2}$) is demonstrated by sample ZC3, obtained at low concentration of zinc nitrate and high concentration of cobalt nitrate. Sample ZC4, similar to ZC3 in terms of Zn:Co ratio but with higher concentrations of all reagents, also shows high sensitivity: 15.40 $mA \cdot mM^{-1} \cdot cm^{-2}$. This indicates that the high cobalt content of $ZnCo_2O_4$ promotes the formation of active centres that efficiently catalyse glucose oxidation.

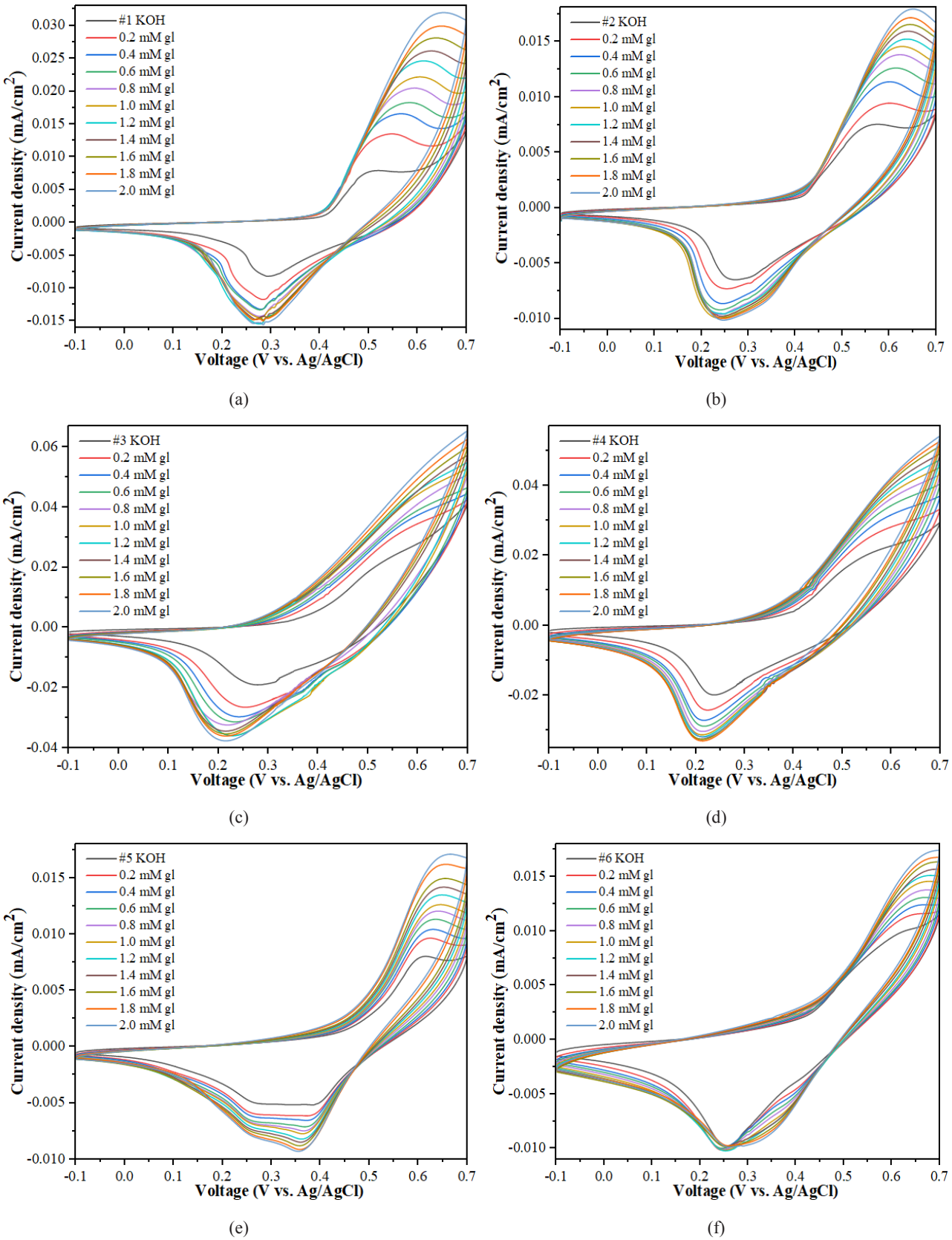

Figure 2 – Cyclic voltammetry patterns of $ZnCo_2O_4$ samples:
(a) ZC1, (b) ZC2, (c) ZC3, (d) ZC4, (e) ZC5, (f) ZC6

In contrast, the samples with excess zinc (ZC5 and ZC6) have the lowest sensitivity: 4.55 and 3.75 $mA \cdot mM^{-1}cm^{-2}$, respectively. This may be due to both less favourable morphology (larger aggregates, lower specific surface area) and lower catalytic activity of Zn-containing phases compared to Co-containing phases. Samples with equimolar ratio of Zn:Co (ZC1 and ZC2) occupy an intermediate position, but at the same ratio the sensitivity decreases with increasing total precursor concentration, possibly due to the densification of the structure and decreased availability of active centres.

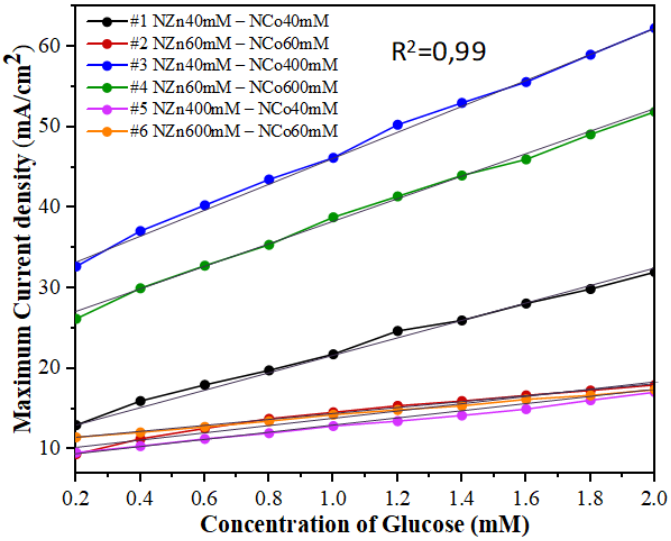

Figure 3 – Plots of variation of peak current density CV at different glucose concentration in alkaline solution of 0.1 M KOH at scanning speed of 25mV/s.

Table 1 – Sensitivity of $ZnCo_2O_4$ samples for glucose detection.

Sample name	Composition of the growth solution	Sensitivity, $mA \cdot mM^{-1} \cdot cm^{-2}$
ZC1	NZn40mM / NCo40mM, urea 100mM	12.05
ZC2	NZn60mM / NCo60mM, urea 150mM	5.25
ZC3	NZn40mM / NCo400mM, urea 100mM	18.65
ZC4	NZn60mM / NCo600mM, urea 150mM	15.40
ZC5	NZn400mM / NCo40mM, urea 100mM	4.55
ZC6	NZn600mM / NCo60mM, urea 150mM	3.75

To obtain more information about the charge transfer efficiency and charge separation at the $ZnCo_2O_4$/Ni interface, electrochemical impedance (EIS) measurement was performed in the range of $0.1 \div 10^5$ Hz at a bias voltage of +0.1 V. Figure 4 shows Nyquist plots between imaginary and real impedance for all $ZnCo_2O_4$ samples of the considered series in 0.1M KOH. The inset of Fig. 4a shows the equivalent Randle circuit, where R1 represents the equivalent series resistance of the electrolyte solution, R2 is the charge transfer resistance and Ws is the Warburg impedance.

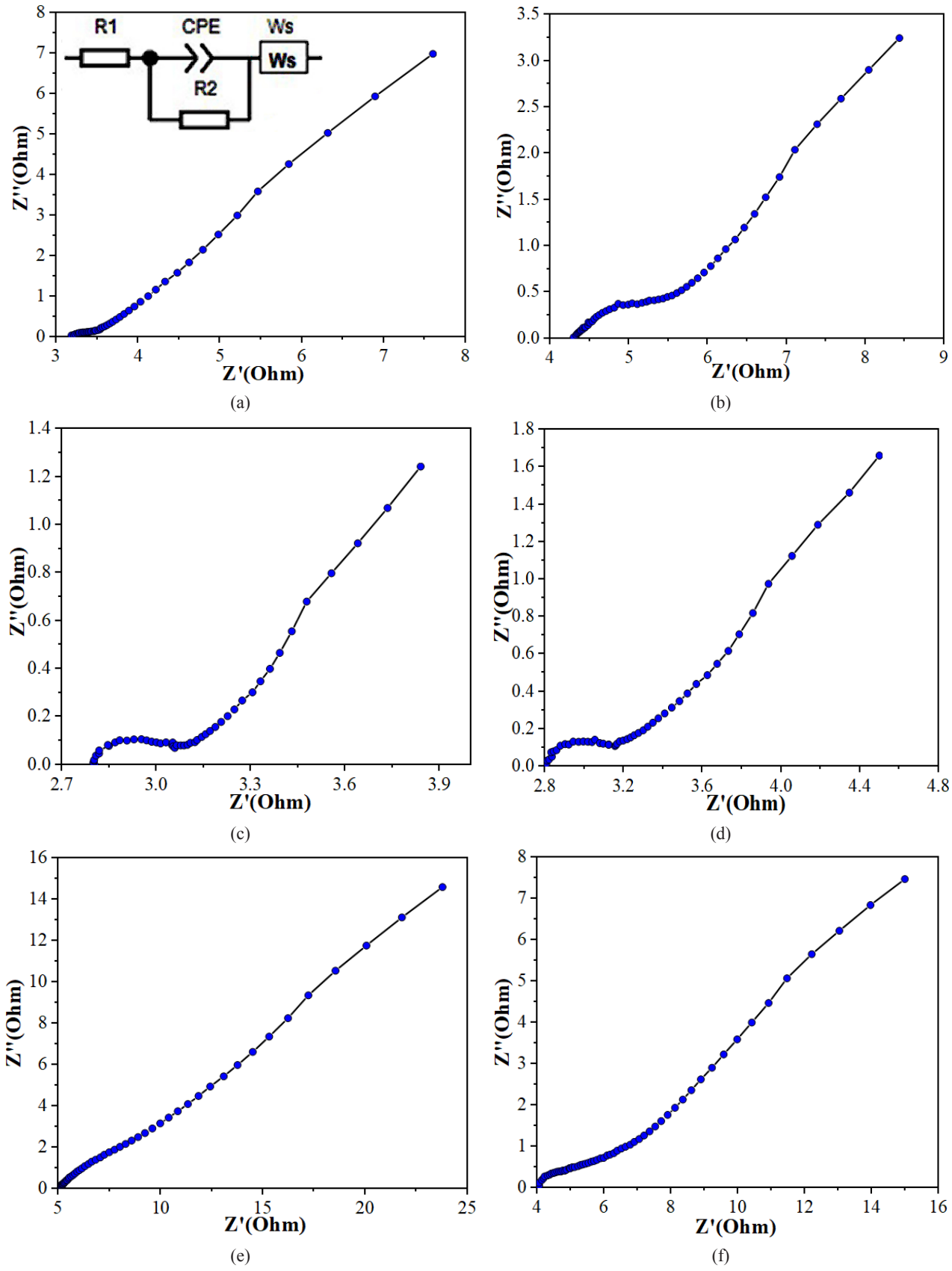

Figure 4 – Nyquist diagrams of $ZnCo_2O_4$ samples:
(a) ZC1, (b) ZC2, (c) ZC3, (d) ZC4, (e) ZC5, (f) ZC6.

CPE (constant phase element) is the circuit element used to describe the capacitance exhibited in real electrochemical systems due to surface roughness or reaction rate distribution. The R2 value for samples ZC2 and ZC4 were compared and found to be 1.21 Ohm and 0.18 Ohm respectively. From Table 1 it can be seen that sample ZC4 with a lower R2 value has a sensitivity 2.5 times higher than sample ZC2. This shows the importance of achieving low R2 values to achieve high sensitivity.

Analysis of Nyquist diagrams shows that all dependences are characterised by the presence of a semicircle in the high-frequency region and a linear section in the low-frequency region. The radius of the semicircle directly correlates with the value of R2: the smaller the radius, the lower the resistance to charge transfer and the higher the kinetics of the electrochemical reaction. The most pronounced small semicircle is observed in the ZC3 sample, indicating the lowest charge transfer resistance among all samples. This is in agreement with the previously obtained cyclic voltammetry data, where sample ZC3 showed the highest sensitivity to glucose. The low R2 indicates high interface conductivity and efficient separation of electron-hole pairs, which is probably due to the high concentration of Co^{3+}/Co^{4+} centres acting as active catalytic sites, as well as favourable morphology promoting rapid charge transfer. The ZC4 sample recorded a close half-circle radius, which also corresponds to a low charge transfer resistance. On the contrary, samples with excess zinc: ZC5 and ZC6 have the largest half-circle radii, indicating high charge transfer resistance and less efficient conduction at the interface, which is consistent with their low sensitivity (Table 1). Apparently, excess Zn^{2+} leads to the formation of less conductive phases or impairs electronic cohesion in the coating, and may also promote particle aggregation, reducing the availability of active centres. Meanwhile, samples with equimolar Zn:Co ratios (ZC1 and ZC2) occupy an intermediate position in terms of half-circle radius value and charge transfer resistance, respectively. The low-frequency linear sections of the diagrams corresponding to the diffusion region also differ in slope. Samples ZC3 and ZC4 show steeper slopes, indicating more efficient mass transfer associated with the diffusion of glucose and OH- ions to the electrode surface, which also confirms their high electrochemical activity.

Thus, the excess of cobalt in the composition promotes the formation of conductive and catalytically active Co^{3+}/Co^{4+} centres, improving the kinetics of the oxidation reaction. The EIS results confirm that controlling the composition of the growth solution allows not only controlling the morphology but also directly influencing the electronic and kinetic characteristics of $ZnCo_2O_4$. The ZC3 sample is of most interest for applications in electrochemical sensors and energy storage devices due to its low charge transfer resistance and high reactivity.

4. Conclusion

The hydrothermal method allowed the preparation of $ZnCo_2O_4$ nanostructures on nickel foam with controlled morphology. Transmission electron microscopy showed that at a molar ratio of Zn:Co = 1:1, uniform nanoparticles with a developed surface are formed. When the zinc content increases, crystallite enlargement and particle aggregation occur, leading to a decrease in the specific surface area of the material. It is shown that the optimal morphological characteristics of $ZnCo_2O_4$ are achieved when the ratio of zinc and cobalt is close to stoichiometric. The electrochemical activity of $ZnCo_2O_4$ nanostructures in the reaction of glucose oxidation in alkaline medium depends significantly on the molar ratio of Zn:Co in the initial growth solution. The samples with excess cobalt (Zn:Co = 1:10) show the highest sensitivity to glucose, which is due to the high catalytic activity of Co^{3+}/Co^{4+} redox couples and, probably, to a more developed surface morphology. Samples with excess zinc show low sensitivity, which is due to the less favourable structure and lower activity of the zinc-containing phases. At higher salt concentrations in the growth solution, a decrease in sensitivity was observed, possibly due to greater particle aggregation. The ZC3 sample (Zn:Co = 40:400 mM) is the most promising for application in non-enzymatic glucose sensors due to its high sensitivity (18.65 $mA \cdot mM^{-1}cm^{-2}$). The electrochemical impedance spectroscopy method showed that the charge transfer resistance R2 depends significantly on the molar ratio of Zn:Co in the growth solution. The lowest R2 was recorded for the ZC3 sample, which correlates with its highest sensitivity to glucose and indicates efficient charge transfer and high catalytic activity.

The results obtained confirm the possibility of controlling the electrochemical properties of $ZnCo_2O_4$ by controlling the composition of the growth solution, which opens prospects for the development of highly sensitive and stable non-enzymatic biosensors based on transition oxides.

Acknowledgements. The study was carried out with the financial support of the Ministry of Science and Higher Education of the Republic of Kazakhstan (grant No AP26103537).

References

1. Liang J., Huang Q., Wu L., Wang L., Sun L., Zhou Zh., Li G. Silicon-based field-effect glucose biosensor based on reduced graphene oxide-carboxymethyl chitosan-platinum nanocomposite material modified LAPS // Sensors and Actuators A: Physical. – 2024. – Vol. 366. – Art. 114937. https://doi.org/10.1016/j.sna.2023.114937

2. Bakranova D., Seitov B., Bakranov N. Photocatalytic and glucose sensing properties of ZnO-based nanocoating// ChemEngineering. – 2023. – Vol. 7. – Art. 22. https://doi.org/10.3390/chemengineering7020022

3. Kumar A., Kumar A., Sagar P., Srivastava M., Pandey A., Prakash R., Srivastava S.K. A sensitive SPR biosensor for glucose detection using MoS_2 quantum dots // Microchemical Journal. – 2025. – Vol. 214. – Art. 113889. https://doi.org/10.1016/j.microc.2025.113889

4. Yojo L.S., Rangel R.C., Duarte P.H., Sasaki K.R.A., Martino J.A. An enzymatic glucose biosensor using the BESOI MOSFET // Solid-State Electronics. – 2024. – Vol. 211. – Art. 108830. https://doi.org/10.1016/j.sse.2023.108830

5. Hamidi H., Murray R., Vezzoni V., Bozorgzadeh S., O'Riordan A., Pontiroli D., Riccò M., Quinn A.J., Iacopino D. A high performance laser induced graphene (LIG) dual biosensor for simultaneous monitoring of glucose and lactate // Biosensors and Bioelectronics: X. – 2025. – Vol. 24. – Art. 100600, https://doi.org/10.1016/j.biosx.2025.100600

6. Ghanbari A.H., Fathi S., Sheikhi M.H., Kordrostami Z. Fabrication of non-enzymatic glucose biosensor based on CuS/Ni_3S_4 reinforced microflowers // Chemosphere. – 2025. – Vol. 382. – Art. 144450. https://doi.org/10.1016/j.chemosphere.2025.144450

7. Jazi H.K., Sarafbidabad M., Henda M.B., Ahmadipour M. The effect of laser surface texturing on ZnO/MWCNT nanocomposite modified screen-printed carbon electrode for non-enzymatic glucose biosensor // Diamond and Related Materials. – 2025. – Vol. 151. – Art. 111845. https://doi.org/10.1016/j.diamond.2024.111845

8. Zhang C., Xu X., Li B., Li H., Tan X., Jesuraj P.J., Xie W. Ultra-sensitive and low detection limitation non-enzymatic glucose biosensor based on heterojunction $NiO@In_2O_3$ hollow nanofibers // Microchemical Journal. – 2025. –Vol. 208. – Art. 112401. https://doi.org/10.1016/j.microc.2024.112401

9. Kalkozova Z.K., Gritsenko L.V., Balgimbayeva U.A., Gabdullin M.T., Wen D., Abdullin Kh.A. New cobalt hydroxycarbonate-based material for highly sensitive enzyme-free glucose sensors // Scientific Reports. – 2025. – Vol. 15. – Art.17154. https://doi.org/10.1038/s41598-025-01164-2

10. Emin A., Ding A., Ali S., Chhattal M., Ali S., Parkash A., Li Q. Electrochemical non-enzymatic glucose biosensors based on Au-thiol-linked molecular architectures // Microchemical Journal. – 2024. – Vol. 207. – Art.111972. https://doi.org/10.1016/j.microc.2024.111972

11. Şavk A., Aydın H., Cellat K., Şen F. A novel high performance non-enzymatic electrochemical glucose biosensor based on activated carbon-supported Pt-Ni nanocomposite // Journal of Molecular Liquids. – 2020. – Vol. 300. – Art. 112355. https://doi.org/10.1016/j.molliq.2019.112355

12. Henry O.E., Hitler L., Udochukwu C.G., Stephen A.A., Ernest C.A., Adedapo S.A. Single-metal (Cu, Ag, Au) encapsulated gallium nitride nanotube (GaNNT) as glucose nonenzymatic nanosensors for monitoring diabetes: Perspective from DFT, visual study, and MD simulation // Journal of Molecular Liquids. – 2023. – Vol. 384. – Art.122209. https://doi.org/10.1016/j.molliq.2023.122209

13. Tuan D.V., Ngan D.T.T., Thao D.V.P., Nguyet N.T., Thuy N.T., Thuy N.P., Thu V.V., Hung V.P., Tam P.D. High-performance nonenzymatic electrochemical glucose biosensor based on AgNP-decorated MoS_2 microflowers // Current Applied Physics. – 2022. – Vol. 43. – Pp. 116-123. https://doi.org/10.1016/j.cap.2022.09.001

14. Mubarakali A., Gopinath S., Parthasarathy P., Kumar U. A., Basha A. A. Highly efficient and sensitive non-enzymatic glucose biosensor based on flower-shaped CuO-colloid nanoparticles decorated with graphene-modified nanocomposite electrode // Measurement. – 2023. – Vol. 217. – Art. 113145. https://doi.org/10.1016/j.measurement.2023.113145

15. Markhabayeva A.A., Moniruddin Md., Dupre R., Abdullin K.A., Nuraje N. Designing of $WO_3@Co_3O_4$ heterostructures to enhance photoelectrochemical performances // The Journal of Physical Chemistry A. – 2020. – Vol. 124. – Pp. 486-491. https://doi.org/10.1021/acs.jpca.9b09173

16. Kalkozova Z.K., Balgimbayeva U.A., Gabdullin M.T., Gritsenko, L.V., Suo G., Abdullin K.A. A facile method for synthesizing cobalt oxide nanoparticles to create a highly sensitive non-enzyme glucose sensor // *Biosensors*. – 2025. – Vol. *15*. – Art. 235. https://doi.org/10.3390/bios15040235

17. Li W.W., Qi H., Wang B.G., Wang Q.Y., Wei S.T., Zhang X.L., Wang Y., Zhang L., Cui X.Q. Ultrathin $NiCo_2O_4$ nanowalls supported on a 3D nanoporous gold coated needle for non-enzymatic amperometric sensing of glucose // Microchim Acta. – 2018. – Vol. 185. – Pp. 1-9. https://doi.org/10.1007/s00604-017-2663-8

18. Ma G.R., Yang M., Li C.Y., Tan H.Y., Deng L., Xie S., Xu F.G., Wang L., Song Y.H. Preparation of spinel nickel-cobalt oxide nanowrinkles/reduced graphene oxide hybrid for nonenzymatic glucose detection at physiological level // Electrochim Acta. – 2016. – Vol. 220. – Pp. 545-553. https://doi.org/10.1016/j.electacta.2016.10.163

19. Yong-Yu L., Ping K., Hong-Qi H., Zhong-Gang L., Gang L., Zheng G., Xing-Jiu H. Porous CuO nanobelts assembly film for nonenzymatic electrochemical determination of glucose with High fabrication repeatability and sensing stability // Sensors and Actuators B: Chemical. – 2020. – Vol. 307. – Art. 127639. https://doi.org/10.1016/j.snb.2019.127639

20. Tian L., He G., Cai Y., Wu S., Su Y., Yan H., Yang C., Chen Y., Li L. Co_3O_4 based non-enzymatic glucose sensor with high sensitivity and reliable stability derived from hollow hierarchical architecture // Nanotechnology. – 2018. – Vol. 29. – Art. 075502. https://doi.org/10.1088/1361-6528/aaa1d2

21. Liu L.J., Wang Z.H., Yang J.H., Liu G.L., Li J.J., Guo L., Chen S.L., Guo Q.H. $NiCo_2O_4$ nanoneedle-decorated electrospun carbon nanofiber nanohybrids for sensitive non-enzymatic glucose sensors // Sens Actuator B Chem. – 2018. – Vol. 258. – Pp. 920-928. https://doi.org/10.1016/j.snb.2017.11.118

22. Xinxin D., Kaili L., Yan X., Mengting Y., Ting G., Jun W. Nonenzymatic electrochemical glucose biosensor constructed by $NiCo_2O_4$@Ppy nanowires on nickel foam substrate // Sensors & Actuators B Chemical. – 2019. – Vol. 292. – Pp.121-128. https://doi.org/10.1016/j.snb.2019.04.107

23. Shewale P.S., Yun K.-S. RGO decorated N-doped $NiCo_2O_4$ hollow microspheres onto activated carbon cloth for high-performance non-enzymatic electrochemical glucose detection // Heliyon. – 2023. – Vol. 9 – Art. e17200. https://doi.org/10.1016/j.heliyon.2023.e17200

24. Kim T.W., Woo M.A., Regis M., Choi K.S. Electrochemical synthesis of spinel type $ZnCo_2O_4$ electrodes for use as oxygen evolution reaction catalysts // J Phys Chem Lett. – 2014. – Vol. 5. – Pp. 2370-2374. https://doi.org/10.1021/jz501077u

25. Li H., Wang L., Guan Y., Su Y., Mu J., Che H., Liu A. Guo Z. Facile solvothermal synthesis of $ZnCo_2O_4/MnO_2$ nanosheets composite with enhanced electrochemical properties as supercapacitor electrodes // Appl. Phys. A. – 2018. –Vol. 124. – Art. 485. https://doi.org/10.1007/s00339-018-1894-9

26. Minaj M.F., Satyajeet S.P., Pramod S.P., Appasaheb P.T. Unleashing the potential of binder-free hydrothermally synthesized marigold-like $ZnCo_2O_4$ for supercapacitors // Journal of Energy Storage. – 2023. – Vol. 74. – Art. 109490. https://doi.org/10.1016/j.est.2023.109490

27. Siyu W., Ning D., Dandan H., Ping W., Yupeng D., Pengcheng X., Yanwei S., Yen W. Synergistic effect of fluorine doping and oxygen vacancies on electrochemical performance of $ZnCo_2O_4$ for advanced supercapacitors and Zn-ion batteries // Acta Materialia. – 2023. – Vol. 257. – Art. 119190. https://doi.org/10.1016/j.actamat.2023.119190

28. Vignesh G., Ranjithkumar R., Devendran P., Nallamuthu N., Sudhahar S., Krishna Kumar M. Nitrogen doped reduced graphene oxide/$ZnCo_2O_4$ nanocomposite electrode for hybrid supercapacitor application // Materials Science and Engineering B. – 2023. – Vol. 290. – Art. 116328. https://doi.org/10.1016/j.mseb.2023.116328

29. Silambarasan M., Ramesh P.S., Geetha D., Ravikumar K., Elhosiny A.H., Algarni H., Soundhirarajan P., Chandekar K.V., Shkir M. A facile preparation of zinc cobaltite ($ZnCo_2O_4$) nanostructures for promising supercapacitor applications // J. Inorg. Organomet. Polym. – 2021. – Vol. 31. – Pp. 3905-3920. https://doi.org/10.1007/s10904-021-02077-z

30. Kedruk Y.Y., Contestabile A., Zeng J., Fontana M., Laurenti M., Gritsenko L.V., Cicero G., Pirri C.F., Abdullin K.A. Morphology effects on electro- and photo-catalytic properties of zinc oxide nanostructures // Nanomaterials. –2023. – Vol. 13. – Art. 2527. https://doi.org/10.3390/nano13182527

31. Tolubayeva D.B., Kedruk Y.Y., Gritsenko L.V. Influence of plasma and heat treatments on the properties of ZnO nanorods // Physical Sciences and Technology. – 2022. – Vol. 9, No. 3-4. – Pp.11-17. https://phst.kaznu.kz/index.php/journal/article/view/287/248

32. Tuan D.V., Ngan D. T.T., Thuy N.T., Lan H., Nguyet N.T., Thu V.V., Hung V.-P., Tam P.D. Effect of nanostructured MoS_2 morphology on the glucose sensing of electrochemical biosensors // Current Applied Physics. – 2020. – 20. – Pp. 1090-1096. https://doi.org/10.1016/j.cap.2020.06.027

33. Abdullin Kh.A., Cicero G., Gritsenko L.V., Kumekov S.E., Markhabaeva A.A. Effect of annealing and hydrogen plasma treatment on the luminescence and persistent photoconductivity of polycrystalline ZnO films // Journal of Applied Physics. – 2017. – 121. – Pp. 245303-1–245303-6. https://doi.org/10.1063/1.4989826

34. Mussabek G., Zhylkybayeva N., Baktygerey S., Yermukhamed D., Taurbayev Y., Sadykov G., Zaderko A.N., Lisnyak V.V. Preparation and characterization of hybrid nanopowder based on nanosilicon decorated with carbon nanostructures // Applied Nanoscience. – 2023. – Vol. 13. – P. 6709–6718. https://doi.org/10.1007/s13204-022-02681-6

35. Mussabek G., Zhylkybayeva N., Lysenko I., Lishchuk P.O., Baktygerey S., Yermukhamed D., Taurbayev Ye., Sadykov G., Zaderko A.N., Skryshevsky V.A., Lisnyak V.V., Lysenko V. Photo- and radiofrequency-induced heating of photoluminescent colloidal carbon dots // Nanomaterials. -2022. -Vol.12. – Art. 2426. https://doi.org/10.3390/nano12142426

36. Mussabek G., Baktygerey S., Taurbayev Ye., Yermukhamed D., Zhylkybayeva N., Zaderko A.N., Diyuk V. E. Afonin S., Yar-Mukhamedova G., Mariychuk R.T., Grishchenko L. M., Kanuchova M., Lisnyak V.V. Surface chemistry and catalytic activity in H_2O_2 decomposition of pyrolytically fluoralkynated activated carbons // RSC Advances. – 2024. – Vol.14. – Art. 29052. https://doi.org/10.1039/d4ra04883k

37. Paltusheva Zh.U., Kedruk Y.Y., Gritsenko L.V., Tulegenova M.A., Syritski V., Abdullin Kh.A. The influence of synthesis parameters and thermal treatment on the optical and structural properties of zinc oxide-based nanomaterials// Physical Sciences and Technology. – 2024. – Vol.11, No.1-2. – Pp. 49-57. https://doi.org/10.26577/phst2024v11i1a6

38. Dmitrieva E.A., Lebedev I.A., Grushevskaya E.A., Murzalinov D.O., Fedosimova A.I., Kemelbekova A.E., Kemelbekova A.E., Kazhiev, Zh. Sh., Zhaysanbayev, Zh. K., Temiraliyev A.T. The effect of deposition technique on formation of transparent conductive coatings of SnO_2 // Physical Sciences and Technology. – 2022. – 9. – Pp. 37-44. https://doi.org/10.26577/phst.2022.v9.i1.05

39. Markhabayeva A.A., Dupre R., Nemkayeva R., Nuraje N. Synthesis of hierarchical WO_3 microspheres for photoelectrochemical water splitting application // Physical Sciences and Technology. – 2023. – 10. – Pp. 33-39 https://doi.org/10.26577/phst.2023.v10.i2.04

40. Tolubayeva D.B., Gritsenko L.V., Kedruk Y.Y., Aitzhanov M.B., Nemkayeva R.R., Abdullin K.A. Effect of hydrogen plasma treatment on the sensitivity of ZnO based electrochemical non-enzymatic biosensor // Biosensors. – 2023. –13. – Art. 793. https://doi.org/10.3390/bios13080793

41. Dong X.C., Xu H., Wang X.W., Huang Y.X., Chan-Park M.B., Zhang H., Wang L.H., Huang W., Chen P. 3D graphene–cobalt oxide electrode for high-performance supercapacitor and enzymeless glucose detection // ACS Nano. – 2012. – Vol. 6. – Pp. 3206–3213. https://doi.org/10.1021/nn300097q

Information about authors:

Gritsenko Lesya Vladimirovna (corresponding author) – PhD, Professor at the Satbayev University (Almaty, Kazakhstan, e-mail: l.gritsenko@satbayev.university).

Kalkozova Zhanar Kanievna – Candidate of Physical and Mathematical Sciences, Associate Professor at the Al-Farabi Kazakh National University (Almaty, Kazakhstan, e-mail: zhanar.kalkozova@kaznu.edu.kz).

Kedruk Yevgeniya Yuryevna – PhD, Assistant Professor at the School of Natural and Social Sciences of the Kazakh-British Technical University (Almaty, Kazakhstan, e-mail: y.kedruk@kbtu.kz).

Paltusheva Zhaniya Urazgalievna – PhD, Senior Lecturer at the Satbayev University (Almaty, Kazakhstan, e-mail: zhaniya.paltusheva@gmail.com).

Mussakhanov Madi Nurzhanuly – student of the Kazakh-British Technical University (Almaty, Kazakhstan, e-mail: madimussakhanov@gmail.com).

Abdullin Khabibulla Abdullaevich – Doctor of Physical and Mathematical Sciences, Professor at the Al-Farabi Kazakh National University (Almaty, Kazakhstan, e-mail: kh.abdullin@physics.kz).